BIOCHEMISTRY
including biophysical chemistry & molecular biology

Article

pubs.acs.org/biochemistry

Peptide-Targeted Delivery of a pH Sensor for Quantitative Measurements of Intraglycosomal pH in Live *Trypanosoma brucei*

Sheng Lin,[†] Meredith T. Morris,[‡] P. Christine Ackroyd,[†] James C. Morris,[‡] and Kenneth A. Christensen*[,†]

[†]Department of Chemistry and [‡]Department of Genetics and Biochemistry, Clemson University, Clemson, South Carolina 29634, United States

ABSTRACT: Studies of dynamic changes in organelles of protozoan parasite *Trypanosoma brucei* have been limited, in part because of the difficulty of targeting analytical probes to specific subcellular compartments. Here we demonstrate application of a ratiometric probe for pH quantification in *T. brucei* glycosomes. The probe consists of a peptide encoding the peroxisomal targeting sequence (F-PTS1, acetyl-CKGGAKL) coupled to fluorescein, which responds to pH. When incubated with living parasites, the probe is internalized within vesicular structures that colocalize with a glycosomal marker. Inhibition of uptake of F-PTS1 at 4 °C and pulse−chase colocalization with fluorescent dextran suggested that the probe is initially taken up by non-receptor-mediated endocytosis but is subsequently transported separately from dextran and localized within glycosomes, prior to the final fusion of labeled glycosomes and lysosomes as part of glycosomal turnover. Intraorganellar measurements and pH calibration with F-PTS1 in *T. brucei* glycosomes indicate that the resting glycosomal pH under physiological conditions is 7.4 ± 0.2. However, incubation in glucose-depleted buffer triggered mild acidification of the glycosome over a period of 20 min, with a final observed pH of 6.8 ± 0.3. This glycosomal acidification was reversed by reintroduction of glucose. Coupling of ratiometric fluorescent sensors and reporters to PTS peptides offers an invaluable tool for monitoring in situ glycosomal response(s) to changing environmental conditions and could be applied to additional kinetoplastid parasites.

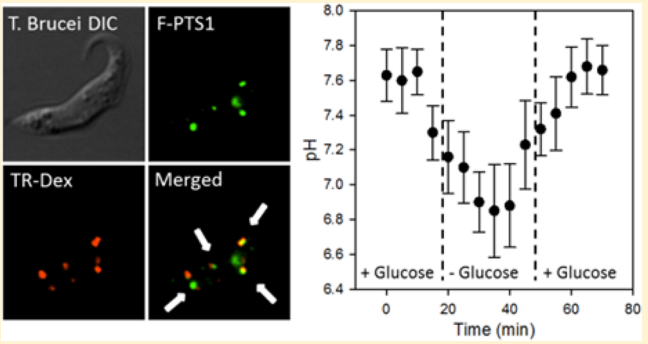

Members of the group Kinetoplastida include the important disease-causing trypanosomatids *Trypanosoma cruzi*, *Leishmania spp.*, and *Trypanosoma brucei*. These unicellular eukaryotic parasites are estimated to infect more than 30 million people a year,[1] with a total of 350 million more at risk for infection worldwide.[2] The current drugs used to treat these infections are often toxic to the host and can be ineffective against certain subspecies or resistant strains of the parasites.[3] To develop more effective therapeutic treatments, a better understanding of trypanosomatid biology is necessary.

Of particular interest are glycosomes, organelles that are evolutionarily related to mammalian peroxisomes, which serve to compartmentalize most of the glycolysis pathway for kinetoplastids. Because proper function of glycosomes is essential for cell survival, it is suggested that they may be an excellent target for drug design.[4,5] One function of the glycosome is to regulate resident enzymes. We have demonstrated that glycosomal enzymes involved in glycolysis, including the essential enzyme hexokinase, are regulated by changes in pH within the organelle in response to environmental changes such as nutrient starvation.[6] This may be analogous to peroxisomally localized enzymes in other organisms responsible for β-oxidation of fatty acids, purine and polyamine catabolism, and amino acid metabolism, which are also pH-dependent.[7] However, despite the importance of glycosomes for kinetoplastid survival and the functional dependence of glycosomal enzymes on solution conditions, relatively little is known about the ionic composition of the glycosomal lumen. Quantitative measurements of the intralumenal environment are required for delineation of glycosome control and function and are therefore required as a necessary step for the design of therapeutics that target glycosomes.

We have devised a strategy for measuring the pH of glycosomes by directing a pH sensitive fluorescent probe with a specific peptide sequence to the glycosomal lumen. Cargo destined for delivery to the glycosome typically harbors a peroxisomal targeting sequence (PTS). PTS type 1 (PTS1) is a C-terminal tripeptide that has been used to transport proteins and other large cargo to the peroxisomal interior in yeast, plants, insects, and mammalian cells.[8−12] PTS sequences have also been fused to fluorescent reporter genes that can be delivered to Trypanosomatid glycosomes.[6,13,14] By coupling PTS1 to fluorescein, a pH reporter dye, we have been able to directly measure the glycosomal pH using fluorescence. The result is the first quantitative measurement of glycosomal pH *in situ*.

Because glycosomes can be fragile structures that lose their integrity upon isolation,[15] the *in vivo* analysis method presented

Received: January 8, 2013
Revised: May 3, 2013
Published: May 7, 2013

here serves as an invaluable research tool. Quantification of glycosomal pH *in situ* and its response to environmental conditions offers important insight into the biochemical properties of the trypanosome metabolic pathway, which can facilitate the development of more effective therapeutics. While the strategy used here is applied to monitor the pH response under conditions of nutrient depletion, peptide-targeted delivery of fluorescent probes can be adapted to study the effects of other developmental and environmental conditions on intracellular solution conditions in *T. brucei* as well as other trypanosomatid and kinetoplastid species.

EXPERIMENTAL PROCEDURES

Reagents. Texas red dextran [TR-Dex, molecular weight (MW) of 10000] and fluorescein dextran (F-Dex, MW of 10000) were obtained from Life Technologies. Fluorescein-tagged peroxisomal transport sequence [F-PTS1, acetyl-C{K-(FITC)}GGAKL; MW of 1107.29] was synthesized by Genscript. Scrambled peptide control [acetyl-LC{K(FITC)}-KGGA; MW of 1107.29] was synthesized by Selleckchem. The immunofluorescence of the glycosome-resident protein hexokinase was performed using the primary antibody α-TbHK (1:500) obtained from P. Michels (Université catholique de Louvain, Brussels, Belgium) and the Texas red-conjugated goat anti-rabbit secondary antibody (1:100) obtained from Rockland Immunochemicals.

Cell Culture and Probe Uptake. *T. brucei brucei* procyclic form (PF) 29-13 parasites were grown in SDM-79 and kept at densities between 5×10^5 and 5×10^7 cells/mL at 28.5 °C in a 5% CO_2 atmosphere.[16,17] For uptake studies, cells were incubated in Voorheis's modified PBS (mPBS) [137 mM NaCl, 3 mM KCl, 16 mM Na_2HPO_4, 3 mM KH_2PO_4, 46 mM sucrose, and 10 mM glucose (pH 7.6)][18] with fluorescent probes [at a final concentration of 90 μM (F-PTS1, scrambled peptide, F-Dex) or 50 μM (TR-Dex)] at 28.5 °C in a 5% CO_2 atmosphere for 1 h.

Flow Cytometry. Cells analyzed by flow cytometry were washed with mPBS three times and then analyzed by cytometry on an Accuri C6 flow cytometer. For each sample, 10000 cells were measured and analyzed with CFlow Plus software (Accuri).

Microscopy. All fluorescent images were acquired on an inverted epifluorescence microscope (Olympus IX71). Differential interference contrast (DIC) was used for transmitted light imaging. The microscope was equipped with both excitation and emission filter wheels (Sutter Instruments). A Sedat filter set consisting of a beam splitter, single-band excitation filters [387 nm (11 nm band-pass), 494 nm (20 nm band-pass), and 575 nm (25 nm band-pass)], and single-band emission filters [447 nm (60 nm band-pass), 531 nm (22 nm band-pass), and 624 nm (40 nm band-pass)] were used for general imaging. For ratiometric imaging of fluorescein, single-band excitation filters [440 nm (20 nm band-pass) and 495 nm (10 nm band-pass)] and single band emission filters [535 nm (25 nm band-pass)] were used. An Orca-ER CCD instrument (Hamamatsu) was used for image acquisition, and all microscope components and all image processing were controlled using Slidebook version 5.0 (Intelligent Imaging Innovations). Fluorescent background signals were determined by average intensities of cell-free regions and subtracted from each image.

Cells used for immunofluorescence (IF) were incubated with 10 mg/mL (0.9 mM) F-PTS1 and washed three times with mPBS. Labeled parasites were then introduced into a perfusion chamber (Harvard Apparatus, Cambridge, MA) and fixed with 4% paraformaldehyde and mPBS (room temperature for 1 h). Cells were then washed with mPBS and permeabilized with 0.1% Triton X-100 in PBS (137 mM NaCl, 3 mM KCl, 16 mM Na_2HPO_4, and 3 mM KH_2PO_4) for 10 min. After the samples had been washed with PBS, blocking buffer (1% BSA and 0.25% Tween in PBS) was added (room temperature for 1 h), followed by addition of α-TbHK (1:500) in blocking buffer for 1 h. Primary antibodies were detected with the Texas red-conjugated goat anti-rabbit antibody (1:100), and images were acquired. All washes were performed with 20−30 chamber volumes at a rate of 50 μL/s.

Lysosomal Colocalization. Qualitative localization analysis of F-PTS1 and TR-Dex was conducted by overnight incubation (28.5 °C in 5% CO_2) of PF *T. brucei* (1×10^7 cells/mL) with TR-Dex (50 μg/mL) in growth medium (SDM-79). Cells were washed three times in mPBS and then incubated with F-PTS1. Cells were then mounted to glass slides, and images were acquired using 494 and 575 nm excitation.

Quantitative localization analysis of co-incubated TR-Dex and F-PTS1 was performed by pulsing cells with both probes in mPBS (50 and 90 μM, respectively) for 1 h, followed by an extended chase with mPBS in the absence of probe. Cells were imaged using 575 and 494 nm excitation at time points over the 320 min chase. The percent colocalization was calculated by creating a segment mask for both emission wavelengths to mark labeled vesicles as mask objects. The lower range of the segment mask was determined by the average emission intensities from the autofluorescence of untreated cells. The number of objects that contained an overlap of both 575 nm (TR-Dex) and 494 nm (F-PTS1) represents regions of colocalization. This overlap number was divided by the total number of objects defined in the 494 nm region to obtain the percent of cellular compartments labeled with F-PTS1 that also colocalize with lysosomal compartments (% $Coloc_{PTS,Lys}$). This relationship can be expressed as

$$\%\mathrm{Coloc}_{\mathrm{PTS,Lys}} = \frac{|\mathbf{M}_{494} \cap \mathbf{M}_{575}|}{|\mathbf{M}_{494}|} \times 100$$

where $\mathbf{M}_{494}$ and $\mathbf{M}_{575}$ are the sets of objects defined by a segment mask at 494 and 575 nm emission, respectively. Defined objects were limited to regions containing higher average intensity than autofluorescence from untreated cells and a size expected for cellular vesicles (between 0.1 and 10 μm^2). Note that because labeled PTS1 and dextran enter the cells through similar mechanisms and that a small fraction of the peptide is either immediately transported to lysosomes or later sent for degradation, it is observed that vesicles that contain both TR-Dex and F-PTS1 objects will be a subset of vesicles containing TR-Dex:

$$(\mathbf{M}_{494} \cap \mathbf{M}_{575}) = \mathbf{M}_{575} \subseteq \mathbf{M}_{494}$$

Statistical analysis of the percent colocalization at each time point was performed with a sample size of 30−60 cells to calculate 95% confidence intervals, based on a normal distribution. Each time point is a representation of several fields taken within 1 min and binned together for analysis.

Intracellular Calibration. Because the fluorescein intensity at 495 nm is sensitive to solution pH while the signal at 440 nm is pH-independent, the intracellular 495 nm/440 nm excitation ratio can be used to monitor intracellular pH, after appropriate

probe calibration. Cells used for intracellular pH calibration were first pulsed with F-PTS1 in mPBS and then mounted in a microscope perfusion chamber. The incubation buffer containing F-PTS1 was then replaced with pH calibration buffer (CB) (130 mM KCl, 1 mM $MgCl_2$, 15 mM HEPES, 15 mM MES, and 0.5 mg/mL digitonin), followed by a 20 min equilibration, and subsequent collection of fluorescent images at 495 and 440 nm emission. Data were sequentially obtained in CB at pH 4–7, with buffer exchange through the perfusion chamber and a 20 min incubation for CB at each pH prior to image collection. The correlation of the 495 nm/440 nm excitation ratio with solution pH was then used to calibrate the ratiometric fluorescein response with intracellular pH. Statistical analysis of the emission ratios at each pH was performed with a sample size of 30–60 cells to calculate 95% confidence intervals based on a normal distribution. Each measurement point is a representation of several fields taken within 1 min and binned together.

Nutrient Deprivation Response. Comparison of glycosomal and lysosomal pH values under normal and glucose-deprived growth conditions was performed by pulsing cells with either F-PTS1 or F-Dex in normal mPBS (containing 10 mM glucose) or glucose-free mPBS using the standard incubation protocol. Cells were then mounted on glass slides and imaged at 495 and 440 nm. The resulting excitation ratio was quantified by comparison with intracellular calibration. Statistical significance between treatments with mPBS and glucose-free mPBS was compared by a one-way analysis of variance (ANOVA).

Monitoring the pH response to glucose deprivation in live PF *T. brucei* was performed by first pulsing the cells with F-PTS1 using the standard incubation protocol. After uptake, cells were washed and placed in a microscope perfusion chamber with fresh mPBS (10 mM glucose). Images were acquired at 495 and 440 nm over 15 min followed by buffer exchange with glucose-deprived mPBS (0 mM). Cells were imaged for an additional 30 min followed by another buffer exchange to normal mPBS (10 mM) and further monitoring. Because the peptide is ultimately delivered to the lysosome, fluorescent compartments containing emission ratios consistent with lysosomal compartments (490 nm/440 nm ratios of <1.2; pH <5.5) were excluded from analysis. Statistical analysis of pH for each measurement was done with a sample size of 30–60 cells to calculate 95% confidence intervals based on a normal distribution. Each measurement point is a representation of several fields taken within 1 min and binned together.

RESULTS

We have previously observed qualitative pH changes inside the glycosomes of *T. brucei* deprived of glucose and proline.[6] With the goal of quantifying those pH changes, we targeted the ratiometric pH sensitive dye fluorescein to the glycosomes using the tripeptide sequence PTS1. Specifically, a fluorescein-tagged peroxisome targeting sequence [F-PTS1, acetyl-C{K-(FITC)}GGAKL] was used, similar to what has been previously applied for peroxisome localization in mammalian cells.[11] Additional modifications included incorporation of two glycine residues to serve as a spacer between the PTS1 sequence and the lysine residue used as the coupling site for the fluorescein moiety. Here we examine the cellular uptake of F-PTS1 and its ability to report pH changes in *T. brucei* glycosomes.

Loading of Procyclic Form (PF) *T. brucei* with F-PTS1. To determine whether the F-PTS1 probe could be adapted as an analytical tool to visualize and quantify intracellular processes in *T. brucei*, we first performed experiments to examine the uptake response in live cells. Because fetal bovine serum in growth medium binds to the peptide and interferes with cellular uptake,[11] incubations were performed in mPBS. Various incubation conditions and probe concentrations were explored (probe loading concentrations of 1 μM to 4.5 mM and incubation times of 10 min to 12 h), with optimal signal to background observed using 90 μM probe in a 60 min incubation. As shown in Figure 1A, incubation with F-PTS1

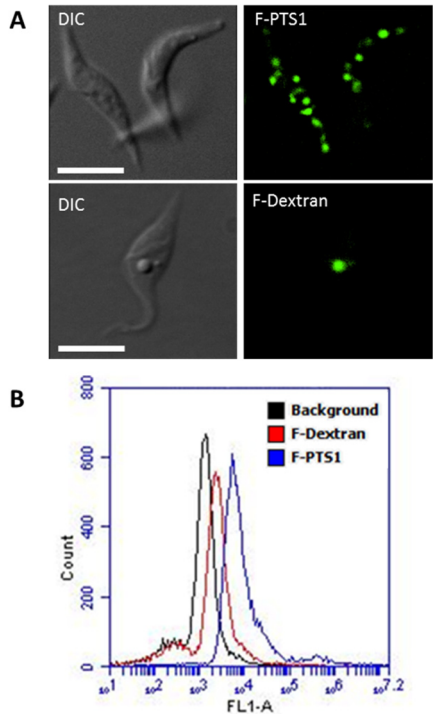

Figure 1. F-PTS1 and F-Dex uptake in live PF *T. brucei*. (A) DIC and fluorescent images of F-PTS1 and F-Dex control. Scale bars are 10 μm. (B) Flow cytometry analysis of F-PTS1, F-Dex, and untreated cells. Incubations were performed with the respective fluorescent probe at 90 μM in mPBS (60 min at 28.5 °C in 5% CO_2). Flow histograms represent fluorescent signals from 10000 live cells.

resulted in a punctate distribution throughout the cells. As a control, incubations under the same conditions were also performed with F-Dex as a bulk-phase endocytic marker; dextran dye conjugates are known to be taken up by host cells via fluid-phase endocytosis and accumulate in lysosomes.[19] Unlike the peptide, F-dex was observed to be sequestered within a single vesicle, consistent with lysosomal localization documented previously in the studies of *T. brucei* dextran uptake.[19]

Flow cytometry was also used to measure the fluorescence per cell of F-Dex and F-PTS1 (Figure 1B). At a loading concentration of 90 μM, cells with F-PTS1 were approximately 10 times brighter than F-Dex control and 50 times brighter than background. This suggests that F-PTS1 and dextran conjugates are transported differently, which is consistent with the expected transport of F-PTS1 to glycosomes. Moreover, these data indicate that trafficking of F-PTS1 results from the PTS1 sequence, not from any characteristics of fluorescein.

dx.doi.org/10.1021/bi400029m | *Biochemistry* 2013, 52, 3629–3637

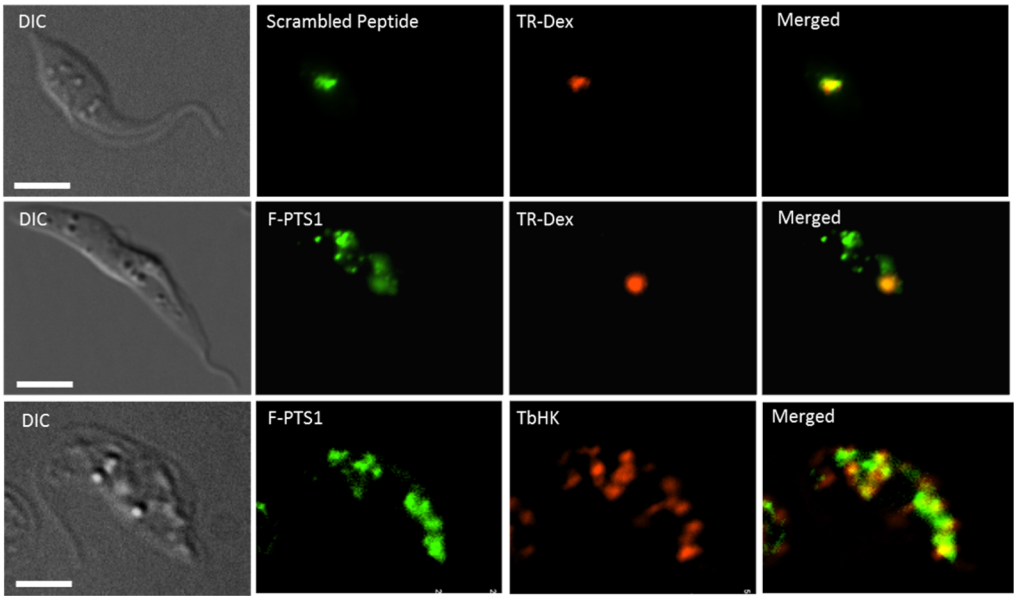

Figure 2. Localization of the scrambled peptide with TR-Dex (top), F-PTS1 with TR-Dex (middle), and TbHK1 (bottom) in PF *T. brucei*. Cells were incubated with 90 μM scrambled peptide or F-PTS1 in mPBS (60 min at 28.5 °C in 5% CO_2). Analysis of colocalization with lysosomal compartments was conducted with cells preloaded with 50 μM TR-Dex overnight in growth medium. Analysis of F-PTS1 colocalization with glycosomes was conducted using immunofluorescence with α-TbHK1 and Texas red-conjugated secondary antibody following F-PTS1 incubation. Scale bars are 5 μm.

When cells were incubated with F-PTS1 at 4 °C, no intracellular fluorescence was observed, indicating that the peptide failed to cross the cellular membrane at low temperatures. Intracellular fluorescein fluorescence was absent in chilled cells even at higher loading concentrations (1−5 mM) and increased incubation times (up to 4 h). Because endocytosis is inhibited at low temperatures,[20] the lack of uptake at low temperatures implies that cellular entry occurs by an active endocytic process. We also observed no labeling of the cellular membrane under low-temperature conditions, suggesting that direct binding of F-PTS1 to cell surface receptors or specific surface proteins does not occur. Hence, the endocytic process is not prompted to direct binding of F-PTS1 to extracellular receptors.

Localization Analysis of F-PTS1 with Subcellular Compartments. While the uptake pattern and fluorescence of F-PTS1 in *T. brucei* were distinct from those of the F-Dex controls, indicating that F-PTS1 is transported in a manner that is independent of F-Dex, further experiments were necessary to determine the identity of the subcellular compartment(s) harboring the peptide probe. To follow F-PTS1 trafficking, and more specifically localize the probe, we performed colocalization experiments with TR-Dex and F-PTS1. Parasites were first loaded with TR-Dex overnight, to allow sufficient time for the dextran dye conjugate to be taken up by host cells by fluid-phase endocytosis and to accumulate in lysosomes.[19] These dextran-loaded cells were then subjected to further incubation with F-PTS1 for localization analysis (Figure 2). Cells containing F-PTS1 and TR-Dex yielded a single doubly labeled focus reflecting the presence of both fluorescent probes, as well as many compartmentalized regions that contained only the labeled peptide. This result suggested that, as seen with TR-Dex, F-PTS1 is able to enter the cell through via endocytosis and is then transported to the lysosomal compartment, along with TR-Dex. However, the peptide apparently reached nonlysosomal compartments as well, either by escaping the endosomal maturation pathway or by entering the cell through a second distinct mechanism.

This observation is in contrast to those made during control experiments performed with a scrambled peptide sequence [acetyl-LC{K(FITC)}KGGA]. This sequence contains the same amino acids, acetylation, and fluorescent labeling of F-PTS1 but lacks the AKL sequence used by the cell for glycosome trafficking. When the scrambled peptide (Figure 2) is incubated with the cells, it is transported only to lysosomes and not to additional compartments, unlike F-PTS1.

To determine the identity of the nonlysosomal compartment in which the F-PTS1 was found, immunofluorescence (IF) with organelle-specific markers was performed. Parasites were first preloaded with F-PTS1 and fixed. Because of the low number of amines in the PTS peptide, standard IF fixation methods could not adequately maintain the spatial distribution of the peptide during IF sample processing. To address this issue, a modified sample preparation was used in which the cells were mounted and washed within a microscopic perfusion chamber. While permeabilization, blocking, and labeling steps followed standard IF procedures (described in Experimental Procedures), the use of a perfusion chamber eliminated the need to adhere the cells to the slide. Additionally, this setup facilitated rapid buffer exchange, which decreased sample preparation time and minimized leakage of the peptide from compartments in which it was sequestered. Glycosomes were identified using antisera to the glycosome-resident TbHKs. While the localization of F-PTS1 is slightly diffuse because of the challenges of fixing the peptide, the peptide can be seen to colocalize with the TbHK marker for glycosomes. This result supports the hypothesis that the probe is successfully transported to glycosomes. It has been documented that mature peroxisomes are no longer PTS import competent,[12,15] which may also be the same for glycosomes. Thus, while the peptide is mostly seen to overlap with TbHK, it is observed and expected that not all the TbHK is colocalized with F-PTS1.

dx.doi.org/10.1021/bi400029m | *Biochemistry* 2013, 52, 3629−3637

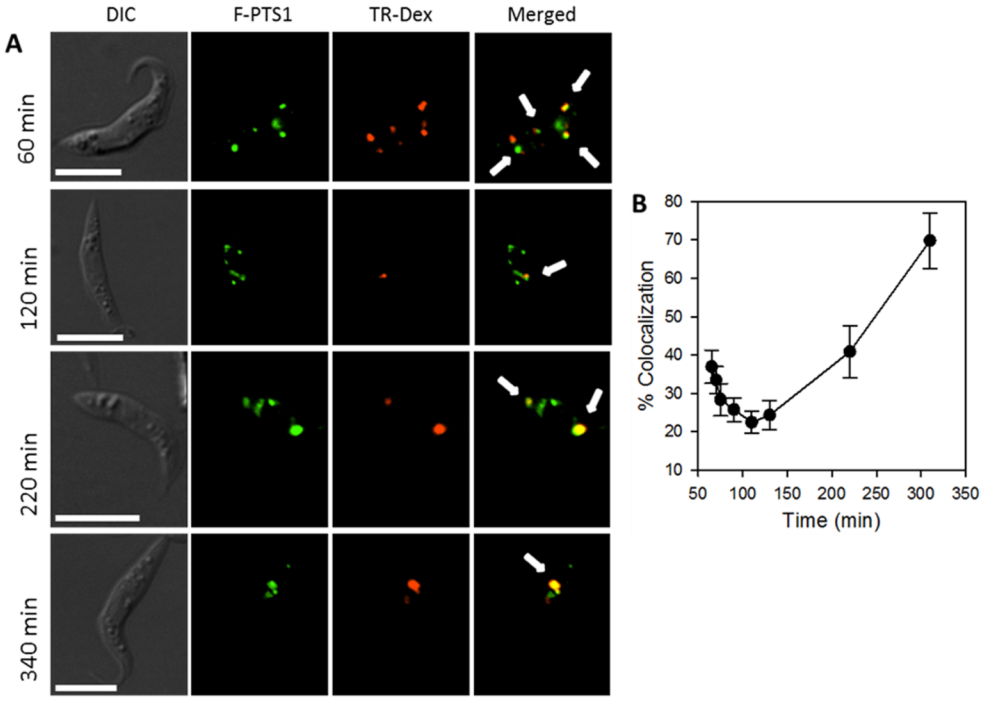

Figure 3. Pulse–chase localization of co-incubated F-PTS1 and TR-Dex in PF *T. brucei*. (A) DIC, F-PTS1, TR-Dex, and merged fluorescent images at various time points over 340 min. White arrows represent points of colocalization. Scale bars are 10 μm. (B) Quantification of the percent of compartmentalized F-PTS1 colocalized with TR-Dex at various time points over 320 min. Cells were co-incubated with 90 μM F-PTS1 and 50 μM TR-Dex in mPBS (28.5 °C in 5% CO_2) for 1 h followed by copious washing and replacement with fresh buffer. Colocalization analysis was completed via fluorescence microscopy. Error bars represent 95% confidence intervals of 30–60 cells.

We next began examinations of the endocytic mechanism resulting in the delivery of F-PTS1 to glycosomes. The observation that cells incubated at 4 °C had no visible F-PTS1 uptake suggested that the mechanism of probe uptake and delivery to glycosomes must be endocytosis. Because the probe was observed in both the lysosome and glycosomes, we hypothesized that the peptide may be transported into the cell in a pathway that is common to both lysosome- and glycosome-targeted cargo. This observation in trypanosomes is not unprecedented. Previous studies in which horseradish peroxidase (HRP) and transferrin gold were co-incubated revealed that transferrin gold particles were directed into large lysosomal-like structures while HRP was found both in the lysosome and in tubular structures near the Golgi apparatus.[21] Together, these observations suggest that trypanosomes contain mechanisms for redirecting cargo acquired after endocytic uptake.

To test our hypothesis that F-PTS1 was redirected following co-uptake with dextran, we performed a pulse–chase experiment in which we monitored and quantified the localization of both TR-Dex and F-PTS1. Both probes were first co-incubated with *T. brucei* in mPBS. The cells were then thoroughly washed, mounted on glass slides, and imaged at various time points over 5 h (Figure 3A). The first time point image (60 min) was captured immediately after the cells were transferred to fresh mPBS following the pulse with the fluorescent probes. At this time point, punctate vesicles that harbored either dextran and the PTS1 probe or just the F-PTS1 probe were observed. This result is consistent with simultaneous uptake of dextran and the probe. However, after 120 min, the amount of colocalization decreased. Rather than multiple vesicles labeled with dextran, only one or two were observed in each cell. Because the excess dextran in the initial pulse had been removed by washing, no new Texas red-loaded endosomes were observed and the existing endosomes had likely fused with lysosomes. The observed lysosomal staining was consistent with previous reports noting that *T. brucei* harbor one or two lysosomal compartments in each cell.[22,23] A greatly decreased level of colocalization observed at this time point indicates that at this stage, most of the peptide had been redirected to glycosomes and separated from dextran-labeled compartments, resulting in limited colocalization. After additional incubation, however (220 and 320 min), the PTS1-labeled vesicles became increasingly associated with dextran-labeled compartments, suggesting that glycosome turnover by autophagy was at work.

To further assess the relationship among endocytosis, lysosomes, glycosomes, and F-PTS1 trafficking, F-PTS1 colocalization with TR-Dex was assessed by dividing the number of compartments containing fluorescein (F-PTS1) and Texas red (dextran) by the number containing only fluorescein (F-PTS1). To increase throughput and prevent observation bias, calculations were performed by generation of an automatic segment mask for fluorescein and Texas red emission in which the lower-intensity range was set on the basis of the autofluorescence from untreated cells. The resulting masks were defined as individual objects that represented the fluorescently labeled compartments (see Experimental Procedures). The resulting percent colocalization of F-PTS1 and dextran as a function of time revealed that after a 60 min pulse with both F-PTS1 and TR-Dex, approximately 40% of vesicles containing PTS1 also contained dextran (Figure 3B). While we hypothesize that the peptide and dextran enter the cell through the same endocytic mechanism, cargoes that were internalized during an earlier stage of the incubation period have likely undergone separate trafficking to their respective organelles, resulting in 60% of PTS1 already residing in glycosomes at the

dx.doi.org/10.1021/bi400029m | *Biochemistry* 2013, 52, 3629–3637

time of the first time point measurement. Over time, the percent colocalization of the two probes decreased, over the next 60 min, to approximately 20%. In agreement with the images shown in Figure 3A, the extent of colocalization of peptide and dextran after the 2 h incubation gradually increased, suggesting that glycosomes were merging with lysosomes, presumably as a result of glycosomal autophagy.

Determination of the Glycosomal pH. After confirming the subcellular localization of the peptide probe, we proceeded to quantify the pH of glycosomes using the pH sensitive properties of fluorescein. Fluorescein emission is ratiometrically sensitive to pH. Fluorescence emission at 525 nm changes as a function of pH upon excitation at 495 nm but is pH independent upon excitation at 440 nm. By using the 495 nm/440 nm excitation ratio and an intracellular calibration, quantitative pH measurements can be performed without having to consider imaging issues such as photobleaching, differences in the focal plane, or loading concentrations. We first conducted an *in situ* calibration using parasites preloaded with F-PTS1. These cells were mounted in a perfusion chamber to allow rapid buffer exchange with pH calibration buffers (pH 4−8). To permeate the cell and glycosomal membrane, 0.5 mg/mL digitonin, the amount required to compromise the membrane,[24] was added with each calibration buffer. Once the internal pH reached equilibrium, the emission intensity at 495 and 440 nm was acquired. Because the probe is known to also be transported to lysosomes [as shown with TR-Dex colocalization (Figure 2)], compartments with emission ratios correlating to a pH of <5.0 (approximately 5−10% of measured compartments) were omitted. The resulting intracellular calibration was consistent with previous studies of fluorescein *in situ* within lysosomes of mammalian and trypanosome cells (Figure 4).[22,25] The precision of fluorescein in its linear range (pH 5.0−7.5) is within 0.1 pH unit at a 95% confidence interval (CI) and is insignificant when compared to the variation between cells. Using this calibration, we report a pH of 7.4 ± 0.2 (n = 42; mean ± 95% CI) in glycosomes of live *T. brucei* under standard growth conditions. Furthermore, because F-PTS1 is also transported to lysosomes, we were able to determine the pH of that organelle to be 4.5 ± 0.4 (n = 35; mean ± 95% CI). This value is consistent with previous reports of the lysosomal pH in *T. brucei*.[26] However, the pK_a of fluorescein (6.4) limits sensitivity and therefore accuracy at lower pH; our measured uncertainty at this pH may be an underestimate.

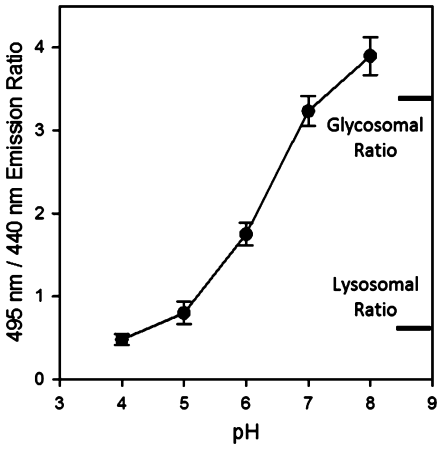

Figure 4. Internal pH calibration of fluorescein in PF *T. brucei* glycosomes. Emission ratios of glycosome-localized F-PTS1 (incubation in mPBS at 90 μM for 60 min at 28.5 °C in 5% CO_2) at 495 and 440 nm are plotted as a function of pH. The internal pH was equilibrated with external pH 4−8 calibration buffers and 0.5 mg/mL digitonin detergent. Markers on the right side represent the emission ratio of fluorescein in live PF *T. brucei* glycosomal (pH 7.4 ± 0.2; n = 42) and lysosomal (pH 4.5 ± 0.4; n = 35) compartments under physiological conditions. Error bars represent 95% confidence intervals of 30−60 cells. Emission ratios were acquired via fluorescence microscopy. We note that the pH-independent 495 nm emission is an internal negative control that corrects for possible signal changes other than pH.

Glycosomal pH Response to Nutrient Deprivation. Previous studies have suggested that glycosomes undergo acidification, with one consequence being the regulation of resident enzymes.[6] One known trigger of qualitative glycosomal acidification is nutrient starvation. For quantitative determination of the effects of starvation on the organellar pH, we measured the consequences of changing glucose availability on the probe excitation ratio.

First, we measured the pH of *T. brucei* glycosomes after incubation in mPBS supplemented with glucose (10 mM) and compared this value to that for cells incubated in the absence of the carbon source (Figure 5A). In the presence of physiological levels of glucose, inner glycosomal pH is equal to the measurements made previously [7.4 ± 0.2 (Figure 4)]. However, in a glucose-deprived buffer, the pH was decreased to 6.8 ± 0.3 (n = 30; mean ± 95% CI). This process was also monitored by a chase experiment (Figure 5B) in which the removal of glucose demonstrates that the acidification process occurs over 20 min. Addition of glucose back to the buffer reversed the acidification over the same duration. This acidification of glycosomes in response to glucose deprivation was found to be statistically significant by ANOVA (p < 0.001), whereas the lysosomal pH under these conditions was not significantly altered. We note that proline is a potential alternate energy source, particularly for procyclic trypanosomes. Because no proline was added to these solutions, the observed glycosomal pH response(s) to glucose deprivation may in fact reflect general starvation conditions, rather than a glucose-specific effect.

DISCUSSION

The studies of F-PTS1 uptake, dextran localization, and immunofluorescence with a glycosomal marker strongly suggest the peptide probe developed here was targeted to glycosomes. While the punctate pattern is consistent with those observed in mammalian studies that target fluorescent probes to peroxisomes using targeting peptide conjugates,[10] the uptake mechanism is likely to be different. When incubation of F-PTS1 was performed at 4 °C, we did not observe uptake, in contrast with previous studies of cellular uptake of PTS-conjugated fluorescein in mammalian cells.[11,27] One reason for this observation may be the different composition of phospholipids in the trypanosomal membrane[28,29] relative to that of mammalian cells, which may reduce the trypanosome cell membrane permeability to extracellular molecules and instead require molecules to enter through a deep invagination of the plasma membrane near the flagella, known as the flagellar pocket.[30] Uptake through the flagellar pocket occurs via a mechanism similar to that found in clathrin-coated vesicle formation in mammalian cells.[31] Given that in mammals, clathrin-coated vesicle formation is sensitive to temperature,[32]

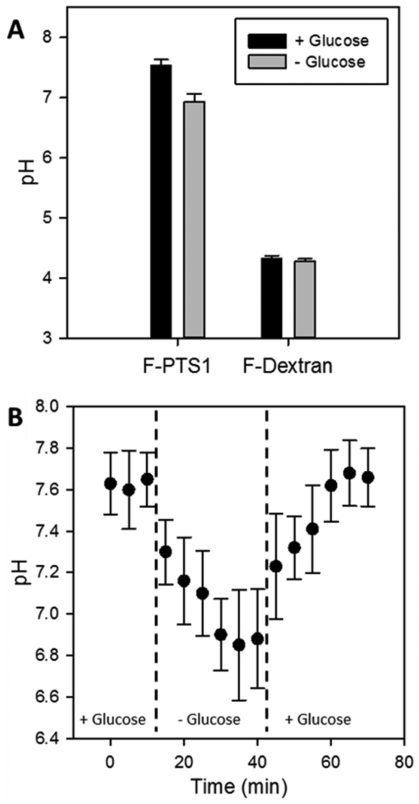

Figure 5. pH response of glycosomes in live PF *T. brucei* to the presence and absence of glucose in incubation buffer. (A) pH difference measured from glycosomal F-PTS1 and lysosomal F-Dex in the presence (black) and absence (gray) of glucose in incubation buffer. Cells were measured after a 60 min incubation (28.5 °C in 5% CO_2) in normal and glucose-deprived mPBS. pH differences of F-PTS1 under the incubation conditions are significantly different as determined by ANOVA ($p < 0.001$) but not for F-Dex control ($p = 0.021$). (B) Glycosomal pH response to glucose deprivation. Glucose removal and addition were performed through buffer exchange of 0 and 10 mM glucose mPBS in a perfusion chamber mounted with live PF *T. brucei* cells. Vertical dotted lines represent time points of buffer exchange. The pH was monitored at 5 min intervals. All pH values were calculated from the 495 nm/440 nm emission ratio of fluorescein with an intracellular calibration. Error bars in both figures represent 95% CIs of 30–60 cells.

operation of the corresponding parasitic mechanism may explain our observation of a low level of peptide uptake in chilled parasites. Uptake by endocytosis also explains why the peptide was observed within trypanosome lysosomes early in the time course of uptake. In contrast, PTS1 peptides in mammalian models enter the cell by passive diffusion and therefore do not accumulate in the lysosomal compartment.

Monitoring both dextran and F-PTS1 uptake together further supported the possibility that trypanosome F-PTS1 uptake was distinct from the mammalian mechanism. We observed that both the peptide probe and dextran were taken up initially by the same endocytic mechanism, only to be later directed to different organelles. Because the first time point represents a 60 min pulse, compartments containing both dextran and peptide may be early endosomes that formed relatively late during the 60 min incubation. Consequently, compartments bearing only peptide may have already been transported to glycosomes. Notably, the overall amount of colocalization gradually decreased during the time course, once the cells were placed into fresh buffer and no new probe uptake could occur. This decrease in the level of colocalization paralleled a decrease in the total number of dextran-labeled compartments, which is likely due to the maturation of early endosomes followed by fusion with lysosomes. It is interesting to note that small amounts of F-PTS1 were directed to a lysosomal compartment. The presence of F-PTS1 in lysosomes may be due to the saturation of the cellular mechanism responsible for directing the peptide or to a regulation mechanism that limits the amount to be imported. Following the segregation of F-PTS1 and dextran, the two markers were observed to gradually merge over the next several hours. This observation is likely due to glycosome turnover by autophagy. While autophagy has been found to occur during the transformation of PF to BSF, low levels of turnover also occur throughout the cell's lifetime to degrade and recycle glycosomal proteins.[33,34] The data reported here suggest that the glycosome's lifetime is approximately 2–6 h in mPBS, which is significantly shorter than the half-life reported for mammalian CHO cells (at ∼2 days)[35] and *T. brucei* (>16 h)[36] in growth medium. This may be due to the starvation of carbon sources in mPBS. In contrast, similar experiments with a scrambled peptide control did not exhibit trafficking to glycosomes and instead remained in the lysosomes.

Using the fluorescent peptide, we were able to measure the pH inside the glycosome. Because a subset of the probe localized to lysosomes rather than glycosomes, these measurements required careful distinction between probes contained in the two different compartments. In this case, the much greater acidity in the two compartments (pH ∼7.4 in glycosomes and pH ∼4.5 in lysosomes) led to a clear bimodal distribution of the fluorescein signal that allowed segregation of the glycosomal signal for pH determination. The pH of glycosomes from parasites grown under standard conditions (7.4) was found to be slightly more alkaline than the pH reported for peroxisomes in CHO cells (6.92),[10] but lower than the value reported for human fibroblast peroxisomes (pH 8.2).[37]

Conditions of nutrient deprivation resulted in significant reductions in glycosomal pH. Monitoring of trypanosome glycosomes loaded with F-PTS1 in a glucose-deprived environment demonstrated an acidification response resulting in a decrease in pH of approximately 0.8 pH unit, which was complete after 20 min. While enzymes are involved in multiple functions within glycosomes, the primary impact of glucose deprivation is expected to be on glycolysis, because this metabolic process uses glucose as the starting metabolite. It has been shown *ex vivo* that *T. brucei* hexokinase (TbHK1), the enzyme responsible for converting glucose to glucose 6-phosphate within the glycolysis pathway, is inactivated at pH 6.5.[6] Moreover, glucose deprivation activates a complex variety of enzymes that alter the primary energy source from glucose to proline.[38] Hence, the rapid pH response observed from glucose deprivation is likely a consequence of pH-based regulation of glycolytic mechanisms, including hexokinase. However, because this pH response was observed in the absence of proline as well as glucose, we cannot distinguish between the effects of general starvation and glucose deprivation.

These studies of intraglycosomal pH demonstrate the utility of peptide-targeted fluorescent probes for quantitative investigation of the intracellular environment, particularly as a response to external stimuli. The advantages of fluorescent peptide probes for such measurements include the ability to rapidly and nondestructively monitor cellular responses within

subcellular compartments in live cells. By altering the choice of the targeting peptide, we can adapt the methodology for analysis in other subcellular organelles; specific peptides have been successfully used to direct cargo to the mitochondria,[39] Golgi apparatus,[40] and endoplasmic reticulum,[41] in addition to glycosomes. By altering the choice of the fluorescent dye, we can also change the analyte of interest or the range of solution conditions available for investigation. For example, peptides can be linked to pH-ratiometric dyes with different linear response ranges relevant to the organelle of interest, including Oregon Green 488 (pK_a = 4.7) that has a working range suitable for highly acidic compartments such as lysosomes. Solution conditions besides pH can also be investigated using other dyes sensitive to specific analytes. Fluo dyes, for example, bind to cellular calcium with a measurable response that can be used for monitoring Ca^{2+} levels.[42,43]

Besides using our fluorescent peptide to monitor the pH response, we have also presented the potential of these measurements as a method for monitoring autophagy of organelles within trypanosomes. By targeting the fluorescent probe to glycosomes and monitoring its colocalization with lysosomal labels, we were able to follow lysosome−glycosome fusion in real time and determine the glycosomal half-life (Figure 3). This observation of lysosomal fusion could be used as a novel method to study organelle autophagy and could be useful in applications that examine the effects of genetic and chemical manipulations on components of the autophagy pathway in live cells.

AUTHOR INFORMATION

Corresponding Author

*E-mail: kchris@clemson.edu. Phone: (864) 656-0930.

Funding

This work was supported in part by National Institutes of Health Grant 1R15AI075326 to J.C.M.

Notes

The authors declare no competing financial interests.

ABBREVIATIONS

F-PTS, fluorescein peroxisomal targeting sequence; TR-Dex, Texas red dextran; F-Dex, fluorescein dextran; α-TbHK, anti-*T. brucei* hexokinase; mPBS, modified phosphate-buffered saline; CB, calibration buffer.

REFERENCES

(1) Beard, C. B. (2009) Forgotten People, Forgotten Diseases: The Neglected Tropical Diseases and Their Impact on Global Health and Development. *Emerging Infect. Dis. 15*, 510−511.

(2) Barrett, M. P., Burchmore, R. J. S., Stich, A., Lazzari, J. O., Frasch, A. C., Cazzulo, J. J., and Krishna, S. (2003) The trypanosomiases. *Lancet 362*, 1469−1480.

(3) Steverding, D. (2008) The history of African trypanosomiasis. *Parasites Vectors 1*, 3.

(4) Coley, A. F., Dodson, H. C., Morris, M. T., and Morris, J. C. (2011) Glycolysis in the African Trypanosome: Targeting Enzymes and Their Subcellular Compartments for Therapeutic Development. *Mol. Biol. Int. 2011*, 1−10.

(5) Opperdoes, F. R. (1987) Compartmentation of carbohydrate metabolism in trypanosomes. *Annu. Rev. Microbiol. 41*, 127−151.

(6) Dodson, H. C., Morris, M. T., and Morris, J. C. (2011) Glycerol 3-phosphate alters *Trypanosoma brucei* hexokinase activity in response to environmental change. *J. Biol. Chem. 286*, 33150−33157.

(7) Reddy, J. K., and Mannaerts, G. P. (1994) Peroxisomal Lipid Metabolism. *Annu. Rev. Nutr. 14*, 343−370.

(8) Walton, P. A., Gould, S. J., Feramisco, J. R., and Subramani, S. (1992) Transport of microinjected proteins into peroxisomes of mammalian cells: Inability of Zellweger cell lines to import proteins with the SKL tripeptide peroxisomal targeting signal. *Mol. Cell. Biol. 12*, 531−541.

(9) Gould, S. J., Keller, G. A., Hosken, N., Wilkinson, J., and Subramani, S. (1989) A conserved tripeptide sorts proteins to peroxisomes. *J. Cell Biol. 108*, 1657−1664.

(10) Jankowski, A., Kim, J. H., Collins, R. F., Daneman, R., Walton, P., and Grinstein, S. (2001) In Situ Measurements of the pH of Mammalian Peroxisomes Using the Fluorescent Protein pHluorin. *J. Biol. Chem. 276*, 48748−48753.

(11) Dansen, T. B., Pap, E. H. W., Wanders, R. J., and Wirtz, K. W. (2001) Targeted fluorescent probes in peroxisome function. *Histochem. J. 33*, 65−69.

(12) Walton, P. A., Hill, P. E., and Subramani, S. (1995) Import of stably folded proteins into peroxisomes. *Mol. Biol. Cell 6*, 675−683.

(13) Milagros Camara, M. d. L., Bouvier, L. A., Miranda, M. R., and Pereira, C. A. (2012) Identification and validation of *Trypanosoma cruzi*'s glycosomal adenylate kinase containing a peroxisomal targeting signal. *Exp. Parasitol. 130*, 408−411.

(14) Costa-Pinto, D., Trindade, L. S., McMahon-Pratt, D., and Traub-Cseko, Y. M. (2001) Cellular trafficking in trypanosomatids: A new target for therapies? *Int. J. Parasitol. 31*, 536−543.

(15) Subramani, S. (1998) Components involved in peroxisome import, biogenesis, proliferation, turnover, and movement. *Physiol. Rev. 78*, 171−188.

(16) Wang, Z., Morris, J. C., Drew, M. E., and Englund, P. T. (2000) Inhibition of *Trypanosoma brucei* gene expression by RNA interference using an integratable vector with opposing T7 promoters. *J. Biol. Chem. 275*, 40174−40179.

(17) Wirtz, E., Leal, S., Ochatt, C., and Cross, G. A. (1999) A tightly regulated inducible expression system for conditional gene knock-outs and dominant-negative genetics in *Trypanosoma brucei*. *Mol. Biochem. Parasitol. 99*, 89−101.

(18) Nolan, D. P., Jackson, D. G., Biggs, M. J., Brabazon, E. D., Pays, A., Van Laethem, F., Paturiaux-Hanocq, F., Elliott, J. F., Elliot, J. F., Voorheis, H. P., and Pays, E. (2000) Characterization of a novel alanine-rich protein located in surface microdomains in *Trypanosoma brucei*. *J. Biol. Chem. 275*, 4072−4080.

(19) Hager, K. M., Pierce, M. A., Moore, D. R., Tytler, E. M., Esko, J. D., and Hajduk, S. L. (1994) Endocytosis of a cytotoxic human high density lipoprotein results in disruption of acidic intracellular vesicles and subsequent killing of African trypanosomes. *J. Cell Biol. 126*, 155−167.

(20) Fernando, L. P., Kandel, P. K., Yu, J., McNeill, J., Ackroyd, P. C., and Christensen, K. A. (2010) Mechanism of cellular uptake of highly fluorescent conjugated polymer nanoparticles. *Biomacromolecules 11*, 2675−2682.

(21) Webster, P., and Grab, D. J. (1988) Intracellular colocalization of variant surface glycoprotein and transferrin-gold in *Trypanosoma brucei*. *J. Cell Biol. 106*, 279−288.

(22) Brickman, M. J., Cook, J. M., and Balber, A. E. (1995) Low temperature reversibly inhibits transport from tubular endosomes to a perinuclear, acidic compartment in African trypanosomes. *J. Cell Sci. 108* (Part 11), 3611−3621.

(23) Coppens, I., Baudhuin, P., Opperdoes, F. R., and Courtoy, P. J. (1993) Role of acidic compartments in *Trypanosoma brucei*, with special reference to low-density lipoprotein processing. *Mol. Biochem. Parasitol. 58*, 223−232.

(24) Hannaert, V., Albert, M.-A., Rigden, D. J., da Silva Giotto, M. T., Thiemann, O., Garratt, R. C., Van Roy, J., Opperdoes, F. R., and Michels, P. A. M. (2003) Kinetic characterization, structure modelling studies and crystallization of *Trypanosoma brucei* enolase. *Eur. J. Biochem. 270*, 3205−3213.

(25) Poole, B., and Ohkuma, S. (1981) Effect of weak bases on the intralysosomal pH in mouse peritoneal macrophages. *J. Cell Biol. 90*, 665−669.

(26) McCann, A. K., Schwartz, K. J., and Bangs, J. D. (2008) A determination of the steady state lysosomal pH of bloodstream stage African trypanosomes. *Mol. Biochem. Parasitol. 159*, 146−149.
(27) Wendland, M., and Subramani, S. (1993) Cytosol-dependent peroxisomal protein import in a permeabilized cell system. *J. Cell Biol. 120*, 675−685.
(28) Field, M. C., Menon, A. K., and Cross, G. A. (1992) Developmental variation of glycosylphosphatidylinositol membrane anchors in *Trypanosoma brucei*. In vitro biosynthesis of intermediates in the construction of the GPI anchor of the major procyclic surface glycoprotein. *J. Biol. Chem. 267*, 5324−5329.
(29) Richmond, G. S., Gibellini, F., Young, S. A., Major, L., Denton, H., Lilley, A., and Smith, T. K. (2010) Lipidomic analysis of bloodstream and procyclic form *Trypanosoma brucei*. *Parasitology 137*, 1357−1392.
(30) Langreth, S. G., and Balber, A. E. (1975) Protein uptake and digestion in bloodstream and culture forms of *Trypanosoma brucei*. *J. Protozool. 22*, 40−53.
(31) Coppens, I., Opperdoes, F. R., Courtoy, P. J., and Baudhuin, P. (1987) Receptor-mediated endocytosis in the bloodstream form of *Trypanosoma brucei*. *J. Protozool. 34*, 465−473.
(32) Boucrot, E., Saffarian, S., Zhang, R., and Kirchhausen, T. (2010) Roles of AP-2 in Clathrin-Mediated Endocytosis. *PLoS One 5*, e10597.
(33) Schaible, U. E., Schlesinger, P. H., Steinberg, T. H., Mangel, W. F., Kobayashi, T., and Russell, D. G. (1999) Parasitophorous vacuoles of *Leishmania mexicana* acquire macromolecules from the host cell cytosol via two independent routes. *J. Cell Sci. 112* (Part 5), 681−693.
(34) Vickerman, K., and Tetley, L. (1978) Biology and ultrastructure of trypanosomes in relation to pathogenesis. Conference on Recent Advances in the Knowledge of Pathogenicity of Trypanosomes, November 20−23, Nairobi, Kenya.
(35) Huybrechts, S. J., Van Veldhoven, P. P., Brees, C., Mannaerts, G. P., Los, G. V., and Fransen, M. (2009) Peroxisome dynamics in cultured mammalian cells. *Traffic 10*, 1722−1733.
(36) Clayton, C. E. (1988) Most proteins, including fructose bisphosphate aldolase, are stable in the procyclic trypomastigote form of *Trypanosoma brucei*. *Mol. Biochem. Parasitol. 28*, 43−46.
(37) Dansen, T. B., Wirtz, K. W., Wanders, R. J., and Pap, E. H. (2000) Peroxisomes in human fibroblasts have a basic pH. *Nat. Cell Biol. 2*, 51−53.
(38) ter Kuile, B. H. (1997) Adaptation of metabolic enzyme activities of *Trypanosoma brucei* promastigotes to growth rate and carbon regimen. *J. Bacteriol. 179*, 4699−4705.
(39) Omura, T. (1998) Mitochondria-Targeting Sequence, a Multi-Role Sorting Sequence Recognized at All Steps of Protein Import into Mitochondria. *J. Biochem. 123*, 1010−1016.
(40) Kjer-Nielsen, L., van Vliet, C., Erlich, R., Toh, B. H., and Gleeson, P. A. (1999) The Golgi-targeting sequence of the peripheral membrane protein p230. *J. Cell Sci. 112* (Part 11), 1645−1654.
(41) Liu, X., and Zheng, X. F. S. (2007) Endoplasmic Reticulum and Golgi Localization Sequences for Mammalian Target of Rapamycin. *Mol. Biol. Cell 18*, 1073−1082.
(42) Gee, K. R., Brown, K. A., Chen, W.-N. U., Bishop-Stewart, J., Gray, D., and Johnson, I. (2000) Chemical and physiological characterization of fluo-4 Ca^{2+}-indicator dyes. *Cell Calcium 27*, 97−106.
(43) Wahl, M., Lucherini, M. J., and Gruenstein, E. (1990) Intracellular Ca^{2+} measurement with Indo-1 in substrate-attached cells: Advantages and special considerations. *Cell Calcium 11*, 487−500.